

A novel dual-loop feedback scheme with optimized second delay time to suppress spurious tones and timing jitter of self-mode-locked quantum dash lasers emitting at $\sim 1.55 \mu\text{m}$

HAROON ASGHAR* AND JOHN. G. MCINERNEY¹

¹Department of Physics and Tyndall National Institute, University College Cork, Cork, Ireland

*Corresponding author: haroon.asghar@ucc.ie

Compiled June 16, 2022

We demonstrate a novel asymmetric dual-loop feedback scheme to suppress external cavity side-modes induced in self-mode-locked quantum-dash lasers with conventional single and dual-loop feedback. In this letter, we report optimal suppression of spurious tones by optimizing the delay in the second loop. We observed that asymmetric dual-loop feedback, with large ($\sim 8x$) disparity in loop lengths, eliminates all external-cavity side-modes and produces flat RF spectra with low timing jitter compared to single-loop feedback. Significant reduction in RF linewidth and reduced timing jitter was also produced by optimizing delay time in the second feedback loop. Experimental results based on this feedback configuration validate predictions of recently published numerical simulations. This interesting asymmetric dual-loop feedback scheme provides simplest, efficient and cost effective stabilization of optoelectronic oscillators based on mode-locked lasers. © 2022 Optical Society of America

OCIS codes: (140.4050) Mode-locked lasers; (140.5960) Semiconductor lasers; (270.2500) Fluctuations, relaxations, and noise

<http://dx.doi.org/10.1364/ao.XX.XXXXXX>

Semiconductor mode-locked diode lasers (MLLs) are compact, rugged and efficient sources of ultra-short, intense, and high repetition frequency optical pulses with many potential applications such as, all-optical clock recovery, Lidar, optical frequency combs, and telecommunications [1-3]. A major limitation of MLLs for most practical applications is their very high timing jitter and phase noise, as spontaneous emission noise and cavity losses make MLLs prone to broad linewidths and therefore substantial phase noise [4]. To improve timing jitter, several experimental methods such as single cavity feedback [5-8], coupled optoelectronic oscillators (OEOs) [9], hybrid mode-locking [10], injection locking [11,12] and dual-loop feedback [13,14] have been proposed and demonstrated. Of the stabilization techniques demonstrated to date, optical feedback is a promising

approach in which an additional reflector creates a compound cavity with a high quality factor, with no need for an external RF or optical source. Due to the existence of the extra mirror, side-bands resonant with the round trip time of the external cavity are generated which affect the overall timing jitter and quality of the RF spectra. To overcome these issues, optoelectronic feedback [9] can also be utilized to stabilize timing jitter and to suppress cavity side-modes by conversion of the optical oscillation (using a fast photodetector) to an electrical oscillation for use in a long feedback loop. This technique does not require an RF source, but requires optical-to-electrical conversion. Recently, a simpler dual-loop feedback technique [13] without optical/electrical conversion has been demonstrated to improve timing jitter of the MLLs and to filter or suppress the unwanted spurious side-bands. Dual-loop configuration proposed to date [13] yields sub-kHz linewidth but produces additional noise peaks at frequencies resonant with the inverse of the delay time in the second cavity. This is undesirable in many applications where low noise and flat spectra are required, as in frequency comb generation. In order to deal with this problem, an alternative approach is needed. Most recently, the influence of the second feedback delay on side-mode suppression and timing jitter has been studied numerically [15]. In this letter, we report experimental investigation to eliminate these adverse dynamical effects using asymmetric dual-loop feedback by appropriately choosing the length of second feedback cavity. Best side-mode suppression and lower timing jitter relative to single loop feedback was achieved with the length ratio between the two cavities $\sim 8x$. It was further observed that RF linewidth and integrated timing jitter were reduced by increasing the length of the second cavity. Our findings suggest that noise stabilization and side-mode suppression depends strongly on additional feedback delay times in a manner which is predictable and whose control may easily be automated.

Devices under investigation are two-section InAs/InP quantum dash mode-locked laser (QDMLL) with an active layer comprising 9 InAs dash monolayers grown by gas source molecular beam epitaxy (GSMBE) embedded within two barriers and separate confinement heterostructure (SCH) layers (dash in a barrier structure). Both the barriers and SCH layers consisted of

$In_{0.8}Ga_{0.2}As_{0.4}P_{0.6}$ quaternary materials with $\lambda_g = 1.55 \mu\text{m}$ [16]. Total cavity length of each device was $2030 \mu\text{m}$ with absorber lengths of $240 \mu\text{m}$ (length ratio $\sim 11.8\%$), giving pulsed repetition frequency of $\sim 20.7 \text{ GHz}$ ($I_{\text{Gain}} = 300 \text{ mA}$) and showing average free-space output powers of a few mW. Mode-locking was obtained without reverse bias applied to the absorber section, and the heat sink temperature was fixed at 19°C . This is a two-section device but works similar to a single section self-mode-locked laser, since the absorber is not biased; in this case the amount of minimal residual absorption does not affect the mode-locking mechanism [12]. The absorber and gain sections were isolated by a resistance $>10 \text{ k}$. The QDMLL was mounted p-side up on AlN submounts and copper blocks with active temperature control and electrical contacts formed by wire-bonding.

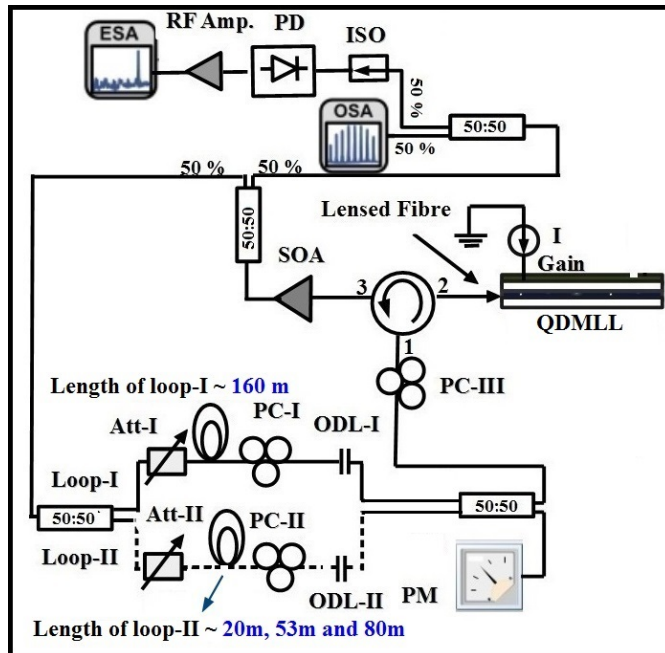


Fig. 1. Schematic of the experimental arrangement for single (excluding dashed portion) and dual-loop configurations (with dashed portion). *Acronyms*– SOA: Semiconductor Optical Amplifier; ISO: Optical isolator; PD: Photodiode; ODL: Optical delay line; Att: Optical attenuator; PC: Polarization controller; ESA: Electrical spectral analyzer; OSA: Optical spectrum analyzer; SMF: Single mode fiber; PM: Power Meter; QDMLL: Quantum dash mode-locked laser

A schematic diagram for the dual-loop technique is depicted in Fig. 1. For single and dual-loop feedback configurations, a calibrated fraction of light was fed back through port 1 of an optical circulator, then injected into the laser cavity via port 2. Optical coupling loss from port 2 to port 3 was -0.64 dB . The output of the circulator was sent to a semiconductor optical amplifier (SOA) with a gain of 9.8 dB , then split into two arms by a $50/50$ coupler. 50% went to an RF spectrum analyzer (Keysight E-series, E4407B) via a 21 GHz photodiode and to optical spectrum analyzers (Ando AQ6317B and Advantest Q8384). The other 50% of power was split into two equal parts by a 3-dB splitter. For a single feedback loop, all power passed through loop-I. For dual-loop configurations (feedback loops-I and-II) the power was split into two loops at the 3-dB splitter. Feedback strengths in both loops were controlled by variable optical

attenuators and monitored using the power meter. In this experimental arrangement, the length of loop-I was fixed to 160 m while the length of second feedback loop was varied in three chosen lengths: 20 , 53 and 80 m . Polarization controllers in each loop plus one polarization controller before port 1 of the circulator ensured the light fed back through both loops matched the emitted light polarizations to maximize feedback effectiveness.

To observe the RF spectrum of single-loop feedback, the length of one feedback loop was fixed to 160 m ; optimally stable resonance occurred when the length of the feedback cavity was optimized using an optical delay line (ODL-I) (which spanned 0 to 84 ps in steps of 1.67 ps). Such optimization yields resonant condition under which the RF linewidth was reduced from 100 kHz for free-running to as low as 4 kHz , with integrated timing jitter to 0.7 ps from 3.9 ps [integrated from $10 \text{ kHz} - 100 \text{ MHz}$]. Measured phase noise traces for free running laser (green line) and single loop feedback (pink line) as functions of frequency offset from fundamental mode-locked frequency are depicted in Fig. 5. Under similar delay settings, external cavity side-modes appear in the RF spectrum with frequency spacing 1.28 MHz , the inverse of the loop round trip delay. RF spectra are shown in Fig. 2(a) (black line) and Fig. 2(b) (black line), using spans of 10 MHz and 100 MHz , respectively. Frequency resonances can be seen in both frequency spans which contribute significantly to timing jitter, particularly for the longer feedback cavities as they are closer to the main peak and are less suppressed [11]. To eliminate these fluctuations and to improve the side-mode suppression ratio (SMSR), dual-loop feedback has been implemented as described in the next section.

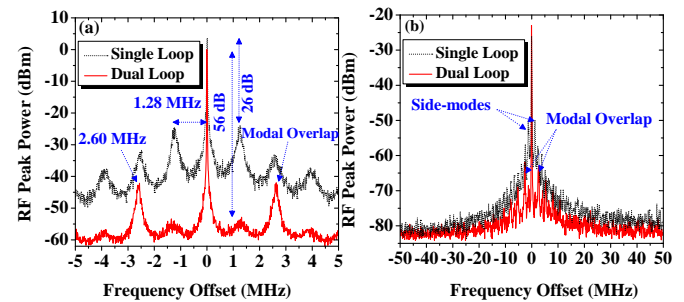


Fig. 2. RF Spectra of single-loop feedback of length 160 m (black line) and dual-loops having lengths 160 m for loop-I and 80 m for loop-II (red line) using frequency span (a) 10 MHz and (b) 100 MHz

To assess the suppression of these frequency resonances, a shorter feedback cavity corresponding to half the period of noise-induced oscillations of loop-I was introduced. The feedback strength from both cavities was kept equal using variable optical attenuators (Att-I and Att-II) plus fine adjustment of polarization controllers (PC-I and PC-II) in both feedback loops. The optical delay (ODL-II) was adjusted to full resonance and the length of optical delay line (ODL-I) was tuned over the maximum range available $0\text{-}84 \text{ ps}$. When the optical delay lines ODL-I and ODL-II were fine tuned so that every second mode of loop-I coincided precisely with a mode of loop-II, maximum $>30 \text{ dB}$ suppression in the first order side-mode was achieved. This optimal suppression of fundamental side-modes occurred due to interference of the two delayed feedback signals at the 3-dB coupler. However, additional noise fluctuations (modal overlap) appear at frequencies resonant with the inverse of the length of second delay time which becomes the carrier signal. These noise fluctuations de-

depends on the ratio of the lengths of two fibers. Here, we noted these fluctuations at frequency spacing 2.60 MHz, consistent with the length of the second feedback loop 80m. RF spectra of asymmetric dual-loop configuration was shown in Fig. 2(a) (red line) and Fig. 2(b) (red line), using spans 10 MHz and 100 MHz, respectively. In this fully resonant configuration, the RF linewidth narrowed to < 1 kHz (instrument limited), with timing jitter reduced to 295 fs. Phase noise traces and minimum RF linewidth are shown in the Fig. 5 (blue line) and Fig. 6 (b) (blue line), respectively. The RF spectra illustrated in Fig. 3(a) and (b) show that this feedback configuration is not suitable to achieve optimal suppression in frequency resonances, as the second delay time will be resonant with the second mode of the first feedback loop which restrict many practical applications where flat and side-band free RF spectrum is required. To improve on this situation, a different dual-loop feedback configuration with non-resonant shorter second loop (53m) is investigated in the next section.

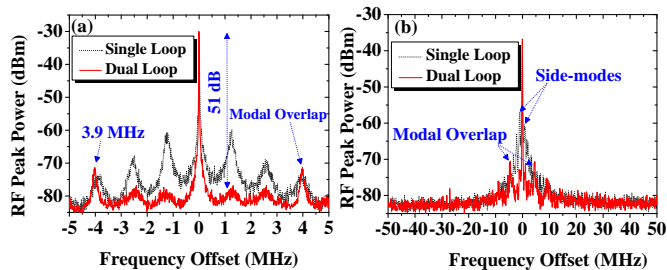


Fig. 3. RF Spectra of single-loop feedback with length 160 m (black line) and dual-loops having lengths 160 m for loop-I and 53m for loop-II (red line) using frequency span (a) 10 MHz and (b) 100 MHz

In the dual-loop configuration presented in this section, the length of loop-I was fixed to 160 m while that of loop-II was kept at 53 m. Upon fine tuning of both optical delay lines, when the second delay time was resonant with the third harmonic of the first loop, suppression of the first two frequency resonances occurred, while the third harmonic (modal overlap) remained unsuppressed. This harmonic was observed at frequency offset 3.9 MHz, corresponding to the 53 m length of the outer feedback loop. RF spectra for the asymmetric dual-loop configuration are shown in Fig. 3(a) (red line) and Fig. 3(b) (red line), using spans 10 MHz and 100 MHz, respectively. In this feedback configuration, when both external feedback cavities are fully resonant then the RF linewidth narrows down to 2 kHz with integrated timing jitter as low as 0.45 ps. Phase noise traces and RF linewidth are shown in inset of Fig. 5 (black line) and Fig. 6 (b) (black line) respectively. These experimentally measured results show that external cavity side-modes cannot be optimally suppressed by simply choosing the second feedback delay time to be a fraction of the first feedback delay time. The optical pulses from the two feedback loops interfere constructively at the 3-dB coupler, producing modal overlap a few MHz away from the fundamental mode-locked frequency which depends on the ratio of the lengths of the two fibers. To eliminate these modal overlaps and to achieve stable and flat RF spectra, a weak mode from the second loop is required, which can be obtained by selecting one feedback loop with short delay time. We therefore designed a novel asymmetric dual-loop feedback configuration in the next section which gives effective suppression in external cavity side-modes and produces lower timing jitter with flat RF

spectra compared to conventional single and dual-loop feedback schemes.

We have implemented a novel asymmetric dual-loop feedback configuration in which the length of loop-I was fixed (160 m) and the length of loop-II was chosen at 8x shorter than loop-I. Separate fine tuning of both external feedback cavities was done to produce precise coincidence of every eighth mode of loop-I with a mode of loop-II, so that strong side-mode suppression occurred and all feedback-induced side-modes and spectral resonances were eliminated. RF spectra for this dual-loop feedback configuration (red line) are shown in Fig. 4. (a) and (b) with frequency spans 10 MHz and 100 MHz respectively. Furthermore, when both external feedback cavities are fully resonant then the RF linewidth narrows to 8 kHz with integrated timing jitter as low as 0.6 ps. The phase noise trace and RF spectra are shown in inset of Fig. 5 (red line) and Fig. 6(b) (red line) respectively. In this configuration, the RF linewidth was higher than for single loop feedback, but measured timing jitter was lower; this is due to suppression of external cavity side-modes. In addition, weak modal overlap in the RF spectrum of dual-loop feedback was noticed at 10 MHz frequency spacing, consistent with our 20 m outer loop; this is shown in Fig. 4(b)(red line). This behavior shows that effective suppression of external cavity side-modes and reduced timing jitter can be achieved by appropriately fine-tuning the length of the second feedback loop.

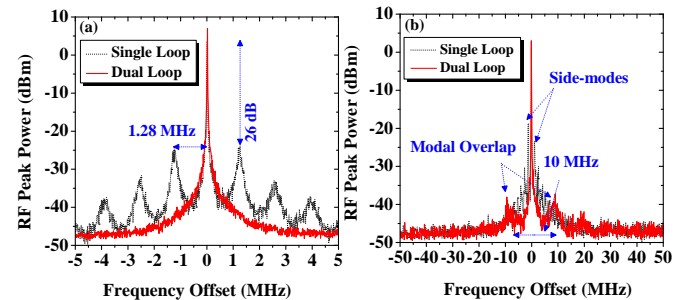


Fig. 4. RF Spectra of single-loop feedback with length 160 m (black line) and dual-loops having lengths 160 m for loop-I and 20 m for loop-II (red line) using frequency span (a) 10 MHz and (b) 100 MHz

In this work, the RMS timing jitter is calculated from the single sideband (SSB) phase noise spectra measured for the fundamental RF frequency (≈ 20.7 GHz) using [8]:

$$\sigma_{RMS} = \frac{1}{2\pi f_{ML}} \sqrt{2 \int_{f_d}^{f_u} L(f) df} \quad (1)$$

where f_{ML} is the pulse repetition rate, f_u and f_d are the upper and lower integration limits. $L(f)$ is the single sideband (SSB) phase noise spectrum, normalized to the carrier power per Hz. To measure RMS timing jitter of the laser in more detail, single-sideband (SSB) noise spectra for the fundamental harmonic repetition frequency were measured. To assess this, RF spectra at several spans around the repetition frequency were measured from small (finest) to large (coarse) resolution bandwidths. The corresponding ranges for frequency offsets were then extracted from each spectrum and superimposed to obtain SSB spectra normalized for power and per unit of frequency bandwidth. The higher frequency bound was set to 100 MHz (instrument limited).

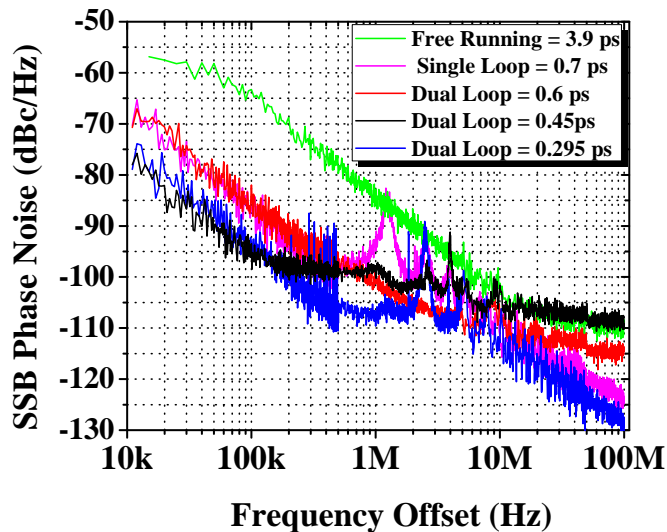


Fig. 5. SSB phase noise trace of free-running, single-loop feedback and dual-loop feedback configurations with loop-I = 160m and loop-II 20, 53 and 80m

Measured phase noise traces for free-running condition (green line), single-loop (pink line) and dual-loop feedback with loop-II at 20m (red line), 53m (black line) and 80m (blue line) as functions of offset from the fundamental mode-locked frequency are given in Fig. 5. A comparison of the RF linewidth and integrated timing jitter under stable resonant condition as functions of three chosen lengths of second feedback cavity is shown in Fig. 6(a). Measured integrated timing jitter in all dual-loop configurations was lower than for single-loop feedback. However, optimal suppression in external cavity side-modes was achieved for the second delay time $\sim 8x$ shorter than first feedback cavity. Furthermore, the integrated timing jitter in this case was 16% lower than single-loop feedback. Reduction in timing jitter occurs due to suppression of all external cavity side-modes in the RF spectra compared to single-loop feedback. In the literature [13], it was experimentally observed that effective side-mode suppression was achieved when the second feedback delay has a common multiple with the first cavity delay. This shows that optimal suppression in external cavity side-modes is highly dependent on the length of the second loop. Recently, the influence of the second loop delay on suppression of external cavity side-modes and timing jitter was studied numerically [15]. In this work, experimental results on suppression of external cavity side-modes and integrated timing jitter as a function of the second cavity delay correspond well with published numerical simulations [15].

In summary, an alternative approach based on asymmetric dual-loop feedback has been demonstrated to suppress additional noise resonances in conventional single- and dual-loop feedback setups. These results show that dual-loop feedback with precise alignment of the second loop delay effectively suppresses external cavity side modes and produces flat RF spectra. Furthermore, by increasing the length of the second loop, significant reduction in RF linewidth and integrated timing jitter was produced. Our experimental results have validated recently published numerical simulations [15]. Using this method, stable and side-band-free integrated photonic oscillators based on mode-locked lasers can be developed which are feasible and attractive for many applications in optical telecommuni-

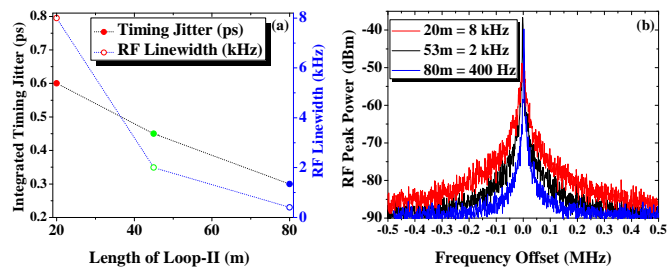


Fig. 6. (a) RF Linewidth (hollow circles) and Integrated timing jitter (solid circles) for dual-loop feedback configurations with loop-I = 160m and loop-II 20, 53 and 80m (b) RF spectrum under stably resonant condition for dual-loop feedback configurations with loop-I = 160m and loop-II 20, 53 and 80m

cations, time-domain multiplexing, frequency comb generation and as synchronized pulse sources or multi-wavelength lasers for wavelength-diversity or multiplexing.

Funding. The authors acknowledge financial support from Science Foundation Ireland (grant 12/IP/1658) and the European Office of Aerospace Research and Development (grant FA9550-14-1-0204).

REFERENCES

- A. Sano, E. Yamada, H. Masuda, E. Yamazaki, T. Kobayashi, E. Yoshida, Y. Miyamoto, R. Kudo, K. Ishihara, and Y. Takatori, *J. Lightwave Technol.* **27**(16), 3705–3713 (2009).
- C. J. Misas, P. Petropoulos, and D.J. Richardson, *J. Lightwave Technol.* **26**(17), 3110–3117 (2008).
- S. Fukushima, C. F. C. Silva, Y. Muramoto, and A. J. Seeds, *J. Lightwave Technol.* **21**(12), 3043–3051 (2003).
- F. Kéfélian, O' Donoghue, M. T. Todaro, J. G. McInerney, and G. Huyet, *IEEE Photonics Technol. Lett.* **20**(16), 1405–1407 (2008).
- O. Solgaard and K. Y. Lau, *IEEE Photonics Technol. Lett.* **5**(11), 1264–1267 (1993).
- C.-Y. Lin, F. Grillot, N. A. Naderi, Y. Li, and L. F. Lester, *Appl. Phys. Lett.* **96**(5), 051118 (2010).
- K. Merghem, R. Rosales, S. Azouigui, A. Akrouf, A. Martinez, F. Lelarge, G.-H. Duan, G. Aubin, and A. Ramdane, *Appl. Phys. Lett.* **95**(13), 131111 (2009).
- D. Arsenijević, M. Kleinert, and D. Bimberg, *Appl. Phys. Lett.* **103**(23), 231101 (2013).
- Y. Cheng, X. Luo, J. Song, T.-Y. Liow, G.-Q. Lo, Y. Cao, X. Hu, X. Li, P. H. Lim, and Q. J. Wang, *Opt. Express.* **23**(5), 6392–6399 (2015).
- V. F. Olle, A. Wonfor, L. A. M. Sulmoni, P. P. Vasilév, J.-M. Lamy, J.-F. Carlin, N. Grandjean, R. V. Penty, and I. H. White, *IEEE Photonics Technol. Lett.* **25**(15), 1514–1516 (2013).
- E. Sooudi, C. D. Dios, J. G. McInerney, G. Huyet, F. Lelarge, K. Merghem, R. Rosales, A. Martinez, A. Ramdane, and S. P. Hegarty, *IEEE J. Sel. Top. Quantum Electron.* **19**(4), 1101208 (2013).
- E. Sooudi, G. Huyet, J. G. McInerney, F. Lelarge, K. Merghem, R. Rosales, A. Martinez, A. Ramdane, and S. P. Hegarty, *IEEE Photonics Technol. Lett.* **23**(20), 1544–1546 (2011).
- M. Haji, L. Hou, A. E. Kelly, J. Akbar, J. H. Marsh, J. M. Arnold, and C. N. Ironside, *Opt. Express.* **20**(3), 3268–3274 (2012).
- O. Nikiforov, L. Jaurigue, L. Drzewietzki, K. Lüdge, and S. Breuer, *Opt. Express.* **24**(13), 14301–14310 (2016).
- L. Jaurigue, E. Schöll, and K. Lüdge, *PRL.* **117**, 154101 (2016).
- F. Lelarge, B. Dagens, J. Renaudier, R. Brenot, A. Accard, F. V. Dijk, D. Make, O. Le Guezou, J. Provost, F. Poingt, J. Landreau, O. Drisse, E. Derouin, B. Rousseau, F. Pommereau, and G. -H. Duan, *IEEE J. Sel. Top. Quantum Electron.* **13**(1), 111–124 (2007).

REFERENCES

1. A. Sano, E. Yamada, H. Masuda, E. Yamazaki, T. Kobayashi, E. Yoshida, Y. Miyamoto, R. Kudo, K. Ishihara, and Y. Takatori, "No-guard-interval coherent optical OFDM for 100-Gb/s long-haul WDM transmission," *J. Lightwave Technol.* **27**(16), 3705–3713 (2009).
2. C. J. Misas, P. Petropoulos, and D.J. Richardson, "All-optical signal processing of periodic signals using a Brillouin gain comb," *J. Lightwave Technol.* **26**(17), 3110–3117 (2008).
3. S. Fukushima, C. F. C. Silva, Y. Muramoto, and A. J. Seeds, "Optoelectronic millimeter-wave synthesis using an optical frequency comb generator, optically injection locked lasers, and a unitraveling-carrier photodiode," *J. Lightwave Technol.* **21**(12), 3043–3051 (2003).
4. F. Kéfélian, O. Donoghue, M. T. Todaro, J. G. McInerney, and G. Huyet, "RF linewidth in monolithic passively mode-locked semiconductor laser," *IEEE Photonics Technol. Lett.* **20**(16), 1405–1407 (2008).
5. O. Solgaard and K. Y. Lau, "Optical feedback stabilization of the intensity oscillations in ultrahigh-frequency passively modelocked monolithic quantum-well lasers," *IEEE Photonics Technol. Lett.* **5**(11), 1264–1267 (1993).
6. C.-Y. Lin, F. Grillot, N. A. Naderi, Y. Li, and L. F. Lester, "rf linewidth reduction in a quantum dot passively mode-locked laser subject to external optical feedback," *Appl. Phys. Lett.* **96**(5), 051118 (2010).
7. K. Merghem, R. Rosales, S. Azouigui, A. Akrouf, A. Martinez, F. Lelarge, G.-H. Duan, G. Aubin, and A. Ramdane, "Low noise performance of passively mode locked quantum-dash-based lasers under external optical feedback," *Appl. Phys. Lett.* **95**(13), 131111 (2009).
8. D. Arsenijević, M. Kleinert, and D. Bimberg, "Phase noise and jitter reduction by optical feedback on passively mode-locked quantum dot lasers," *Appl. Phys. Lett.* **103**(23), 231101 (2013).
9. Y. Cheng, X. Luo, J. Song, T.-Y. Liow, G.-Q. Lo, Y. Cao, X. Hu, X. Li, P. H. Lim, and Q. J. Wang, "Passively mode-locked III-V/silicon laser with continuous-wave optical injection," *Opt. Express.* **23**(5), 6392–6399 (2015).
10. V. F. Olle, A. Wonfor, L. A. M. Sulmoni, P. P. Vasilèv, J.-M. Lamy, J.-F. Carlin, N. Grandjean, R. V. Penty, and I. H. White, "Hybrid and passive mode-locking of a monolithic two-section MQW InGaIn/GaN laser diode," *IEEE Photonics Technol. Lett.* **25**(15), 1514–1516 (2013).
11. E. Sooudi, C. D. Dios, J. G. McInerney, G. Huyet, F. Lelarge, K. Merghem, R. Rosales, A. Martinez, A. Ramdane, and S. P. Hegarty, "A novel scheme for two-level stabilization of semiconductor mode-locked lasers using simultaneous optical injection and optical feedback," *IEEE J. Sel. Top. Quantum Electron.* **19**(4), 1101208 (2013).
12. E. Sooudi, G. Huyet, J. G. McInerney, F. Lelarge, K. Merghem, R. Rosales, A. Martinez, A. Ramdane, and S. P. Hegarty, "Injection-Locking properties of InAs/InP based mode-locked quantum-dash lasers at 21 GHz," *IEEE Photonics Technol. Lett.* **23**(20), 1544–1546 (2011).
13. M. Haji, L. Hou, A. E. Kelly, J. Akbar, J. H. Marsh, J. M. Arnold, and C. N. Ironside, "High frequency optoelectronic oscillators based on the optical feedback of semiconductor mode-locked laser diodes," *Opt. Express.* **20**(3), 3268–3274 (2012).
14. O. Nikiforov, L. Jaurigue, L. Drzewietzki, K. Lüdge, and S. Breuer, "Experimental demonstration of change of dynamical properties of a passively mode-locked semiconductor laser subject to dual optical feedback by dual full delay-range tuning," *Opt. Express.* **24**(13), 14301–14310 (2016).
15. L. Jaurigue, E. Schöll, and K. Lüdge, "Suppression of noise-induced modulations in multidelayer systems," *PRL.* **117**, 154101 (2016).
16. F. Lelarge, B. Dagens, J. Renaudier, R. Brenot, A. Accard, F. V. Dijk, D. Make, O. Le Gouezigou, J. Provost, F. Poingt, J. Landreau, O. Drisse, E. Derouin, B. Rousseau, F. Pommereau, and G.-H. Duan, "Recent advances on InAs/InP quantum dash based semiconductor lasers and optical amplifiers operating at 1.55 μm ," *IEEE J. Sel. Top. Quantum Electron.* **13**(1), 111–124 (2007).